Structural Comparison of Crystal and Solution States of the 138 kDa Complex of Methylamine Dehydrogenase and Amicyanin from *Paracoccus versutus*†

Chiara Cavalieri,‡ Nikolai Biermann,§ Monica D. Vlasie,|| Oliver Einsle,§ Angelo Merli,‡ Davide Ferrari,‡ Gian Luigi Rossi,‡ and Marcellus Ubbink*,||

Department of Biochemistry and Molecular Biology, University of Parma, 43100 Parma, Italy, Institute for Microbiology and Genetics, Georg-August-University Göttingen, Justus-von-Liebig-Weg 11, 37077 Göttingen, Germany, and Leiden Institute of Chemistry, Leiden University, P.O. Box 9502, 2300 RA Leiden, The Netherlands

Received December 5, 2007; Revised Manuscript Received April 4, 2008

ABSTRACT: Methylamine can be used as the sole carbon source of certain methylotrophic bacteria. Methylamine dehydrogenase catalyzes the conversion of methylamine into formaldehyde and donates electrons to the electron transfer protein amicyanin. The crystal structure of the complex of methylamine dehydrogenase and amicyanin from *Paracoccus versutus* has been determined, and the rate of electron transfer from the tryptophan tryptophylquinone cofactor of methylamine dehydrogenase to the copper ion of amicyanin in solution has been determined. In the presence of monovalent ions, the rate of electron transfer from the methylamine-reduced TTQ is much higher than in their absence. In general, the kinetics are similar to those observed for the system from *Paracoccus denitrificans*. The complex in solution has been studied using nuclear magnetic resonance. Signals of perdeuterated, ^{15}N-enriched amicyanin bound to methylamine dehydrogenase are observed. Chemical shift perturbation analysis indicates that the dissociation rate constant is $\sim$250 s^{-1} and that amicyanin assumes a well-defined position in the complex in solution. The most affected residues are in the interface observed in the crystal structure, whereas smaller chemical shift changes extend to deep inside the protein. These perturbations can be correlated to small differences in the hydrogen bond network observed in the crystal structures of free and bound amicyanin. This study indicates that chemical shift changes can be used as reliable indicators of subtle structural changes even in a complex larger than 100 kDa.

The methylotrophs *Paracoccus denitrificans* and *Paracoccus versutus* can grow on methylamine as the sole carbon source, using the enzyme methylamine dehydrogenase (MADH)[1] to convert methylamine into formaldehyde and ammonia. MADH and the blue copper protein amicyanin from *P. denitrificans* have been found to interact in vitro (*1*), and the crystal structure of the binary complex has been determined to 2.5 Å resolution (*2*).

MADH of *P. denitrificans* is a dimer of heterodimers, each one composed of a heavy chain of 43 kDa and a light chain of 14 kDa, the latter containing tryptophan tryptophylquinone (TTQ) as the redox cofactor. TTQ is formed by the covalent linkage of two tryptophan side chains, one of which has been modified to include an orthoquinone function (*3*). Oxidation of methylamine produces the two-electron reduced (aminoquinol) form of TTQ. In the crystal, one amicyanin molecule, with a molecular mass of 12 kDa, binds to each protomer (the heterodimer), via a hydrophobic surface. The distance between the TTQ reactive oxygen (O6) and copper is 16.8 Å, while the distance between the closest TTQ atom and copper is 9.3 Å. In solution, transfer of the first electron from the TTQ aminoquinol (*N*-quinol) to the amicyanin copper is a process activated by monovalent cations and gated by deprotonation of the methylamine-derived amino group (*4*). In the case of the corresponding *O*-quinol, resulting from TTQ reduction by dithionite, electron transfer (ET) is slow and nearly independent of the presence of ions (*5*). It has been established that the dissociation constant of the two proteins is in the micromolar range (*6*).

The structural study of complexes between proteins active in redox reactions aims to provide fundamental information about the recognition mechanisms evolved to optimize transient interactions for intermolecular ET. Numerous examples of such studies have accumulated in recent years, concerning both complexes in solution, investigated by NMR spectroscopy (*7–9*), and crystalline complexes, investigated by high-resolution X-ray crystallography (*10–12*). The latter studies include the ternary complex obtained by cocrystallizing *P. denitrificans* MADH and amicyanin with cytochrome c_{551i}, with a molecular mass of 17.5 kDa (*13, 14*), and the binary complex between the quinoprotein aromatic

† M.U. acknowledges financial support from The Netherlands Organisation for Scientific Research (NWO), Grant 700.52.425. N.B. and O.E. were supported by Deutsche Forschungsgemeinschaft (EI-520/1). G.L.R. acknowledges support by the Ministry of University and Research (MUR), Grant PRIN 2005050270_002.

* To whom correspondence should be addressed. Telephone: +31 71 527 4628. Fax: +31 71 527 4349. E-mail: m.ubbink@chem.leidenuniv.nl.

‡ University of Parma.

§ Georg-August-University Göttingen.

|| Leiden University.

[1] Abbreviations: ET, electron transfer; MADH, methylamine dehydrogenase; TTQ, tryptophan tryptophylquinone; HSQC, heteronuclear single-quantum correlation; NOESY, nuclear Overhauser enhancement spectroscopy; TOCSY, total correlation spectroscopy; TROSY, transverse relaxation-optimized spectroscopy.

10.1021/bi7023749 CCC: $40.75
Published on Web 05/31/2008

amine dehydrogenase (AADH) and azurin from *Alcaligenes faecalis* (*15*). Within the MADH−amicyanin−cytochrome c_{551i} ternary complex, the dehydrogenase and the cupredoxin interact as in their binary complex. The cytochrome binds amicyanin with distances between copper and the nearest atom of the heme of 21 Å and between copper and iron of 24.8 Å. The crystal structures of both the binary and ternary complexes have been used as a basis to propose intermolecular ET pathways (*14, 16*) and to interpret the rates measured in solution (*5, 17, 18*). In the crystal, the ternary complex mediates transfer of methylamine-derived electrons to the heme, as demonstrated by single-crystal polarized absorption microspectrophotometry (*16, 19*) and continuous-wave electron paramagnetic resonance, using polycrystalline powders (*20, 21*). However, ET between the amicyanin copper and the cytochrome is considerably slower than cytochrome reduction in solution in the presence of fully reduced MADH and amicyanin (*19, 20*). AADH is a tetrameric quinoprotein, ~30% identical in sequence to MADH, that transfers electrons from aromatic amines to azurin with a mechanism similar to that of MADH (*22*). In spite of the same chemistry and similar structures of the individual components, upon alignment of the dehydrogenases within the binary complexes, azurin appears to be rotated by 90° with respect to amicyanin (see Figure 6A in ref *15*). The plasticity of this kind of systems is reflected by the nature of the possible electron acceptor which has been suggested to be a cytochrome in the *Methylophilus methylotrophus* W3A1 (*23*) and shown not to be amicyanin in the nonslimy variant W3A1-NS (*24*).

The crystal structure of *P. versutus* MADH (*25, 26*) and both the solution (*27*) and crystal (*28*) structures of amicyanin are known, but the binary complex has not yet been described either in solution or in the crystal.

In this work, the binary complex of *P. versutus* MADH and amicyanin has been characterized both in the crystal and in solution to test the extent of similarity with that obtained from *P. denitrificans*. Functional analysis of the *P. versutus* system yields results that are similar to those obtained for the *P. denitrificans* complex. The crystal structure of the binary complex has been obtained to 2.5 Å resolution and has been compared with the structure of the complex in solution using NMR spectroscopy. By perdeuteration and labeling with ^{15}N, it has been possible to observe amicyanin selectively in this large complex for the first time. Chemical shift perturbation mapping shows good agreement with the interface observed in the crystal and is similar for both redox states of amicyanin. Interestingly, secondary chemical shift effects correlate to differences in the H-bond network observed in the crystal structures of free and bound amicyanin. The combination of NMR and X-ray diffraction demonstrates that these small effects of complex formation far from the interface are significant.

EXPERIMENTAL PROCEDURES

Protein Production and Purification. (i) Amicyanin. Escherichia coli BL21 cells were transformed with the plasmid pET28a-ami (*29*) and cultured at 37 °C in LB medium containing 50 mg/L kanamycin (Sigma-Aldrich, St. Louis, MO). Expression was induced by adding 1 mM isopropyl β-galactoside when the OD_{600} equaled 0.7. After 16 h, the cells were harvested by centrifugation at 6000 rpm for 20 min. Cells were lysed by sonication after adding DNase (Sigma-Aldrich) and 0.5 mM phenylmethanesulfonyl fluoride (Sigma-Aldrich). In the presence of 20 μM $CuSO_4$ to convert apoprotein to holoprotein, $K_3Fe(CN)_6$ was slowly added in amounts sufficient to fully oxidize the bound metal. Holoamicyanin was purified following the published procedure (*30*) with slight modifications. After sonication and centrifugation at 10000 rpm for 30 min, the supernatant was dialyzed overnight in a 3500 MWCO dialysis tube against 2 L of 20 mM sodium phosphate buffer (pH 7) which was replaced twice. The supernatant was then loaded on a DEAE column equilibrated with 20 mM sodium phosphate (pH 7). The protein bound weakly to the column material and could be eluted in the absence of salt. The pH of the protein solution was lowered to 4.5 by slowly adding 50 mM acetate buffer (pH 4.5), and the solution was loaded on a CM column equilibrated with the same buffer. The protein was eluted using a linear gradient (0 to 50%) of 500 mM NaCl in the same buffer and collected as 1.5 mL fractions at a flow rate of 1−1.5 mL/min. Purity was checked by the A_{280}/A_{596} ratio (4.2 for pure protein) (*30*). The yield was 80 mg/L (estimated from $\epsilon = 3900\ M^{-1}\ cm^{-1}$ at 596 nm).

^{15}N-labeled protein was produced as described above, using M9 minimal medium (*31*) supplemented with 1 g/L $^{15}NH_4Cl$. The protein yield after purification was 30 mg/L. [^{15}N,^{13}C]Amicyanin was produced in a minimal medium as described above, but using 2 g/L [$^{13}C_6$] glucose (as the sole carbon source) with a yield of pure protein of 30 mg/L. A minimal medium with D_2O substituting for H_2O and 5 g/L CD_3COONa as the sole carbon source was used to produce [^{15}N,^{2}H]amicyanin (yield after purification, 30 mg/L). Due to possibly incomplete exchange of the amide protons, it was only possible to establish that the deuteration level of nonexchangeable protons was between 83 and 99%, on the basis of mass spectrometry.

(ii) Zn Replacement. Substitution of copper with zinc was performed as described previously (*32*). To remove the unfolded protein, zinc amicyanin was passed through an anionic exchange column (Source 30Q) equilibrated with 20 mM sodium phosphate (pH 7). The protein was eluted with 100 mM NaCl in the same buffer.

(iii) MADH. MADH was expressed in *P. versutus* grown on a minimal medium containing 6.7 g/L Na_2HPO_4, 0.37 g/L KH_2PO_4, 10 g/L $CH_3NH_2 \cdot HCl$, 2 mM $MgSO_4$, a vitamin mix, and a trace elements mix. MADH was purified as previously described (*33*). The MADH purity was indicated by the A_{280}/A_{440} absorption ratio, equal to 6.7 for the pure protein (*33*).

Crystallization. Crystals of the *P. versutus* MADH−amicyanin binary complex were obtained by the hanging drop method. Two microliters of protein solution [9.0 mg/mL MADH and 2.3 mg/mL amicyanin in 0.1 M phosphate buffer (pH 6.5)] were mixed with 2 μL of reservoir solution [28−29.5% PEG 8000, 0.2 M Li_2SO_4, and 0.1 M phosphate (pH 6.5)] and allowed to equilibrate at room temperature. The components of the crystallization medium of this binary complex are totally different from those used to crystallize the corresponding binary complex from *P. denitrificans* (*2*), in particular with respect to the use of PEG instead of a high phosphate concentration.

Table 1: Data Collection and Refinement Statistics[a]

wavelength	0.8414 Å
space group	$P2_12_12_1$
unit cell dimensions	$a = 55.6$ Å, $b = 131.0$ Å, $c = 171.7$ Å, $\alpha = \beta = \gamma = 90°$
resolution limits (last shell)	50.0−2.5 Å (2.6−2.5 Å)
no. of independent reflections	37332 (3897)
completeness	84.1% (80.9%)
multiplicity	3.8 (3.6)
$I/\sigma(I)$	6.51 (2.25)
R_{merge}	0.143 (0.449)
R_{pim}[b]	0.069 (0.224)
R_{free}	0.283
R_{work}	0.235
root-mean-square deviation for bonds	0.012 Å
root-mean-square deviation for angles	1.681°

[a] Values in parentheses are for the highest-resolution shell. [b] R_{pim} according to Weiss and Hilgenfeld (*54*).

Structure Determination. Crystals of the *P. versutus* MADH−amicyanin complex belonged to orthorhombic space group $P2_12_12_1$ with one complete complex per asymmetric unit at a solvent content of 36% and the following unit cell dimensions: $a = 55.6$ Å, $b = 131.0$ Å, and $c = 171.7$ Å. Diffraction data to 2.5 Å resolution were collected on beamline BW7B at EMBL/DESY (Hamburg, Germany), and integration and scaling were carried out using the HKL package (*34*). Phase information was obtained by molecular replacement with MOLREP (*35*), using the coordinates of MADH from *P. denitrificans* (PDB entry 2BBK (*36*)) and amicyanin from *P. versutus* (PDB entry 1ID2 (*28*)) as a search model. Additional model building was done in O (*37*) and Coot (*38*), and CNS (*39*) was used for refinement (Table 1). The coordinates have been deposited in the Protein Data Bank (entry 3C75).

Measurements of Electron Transfer. (i) Reduction of Amicyanin by MADH in Solution. Two-electron-reduced MADH was obtained by exposing the enzyme either to a 3-fold molar excess of methylamine or to 2 mM dithionite. Excess reagent was removed by repeated ultrafiltration on Centricon-30, and complete reduction was confirmed by the characteristic absorption spectrum of the MADH coenzyme (*40*).

The rate of amicyanin reduction was determined by rapidly mixing a solution containing 1 μM reduced MADH (heterotetramer) with a solution containing increasing concentrations of oxidized amicyanin in the range of 10−150 μM in a stopped-flow apparatus. The reaction of methylamine-reduced MADH with amicyanin was studied either in 10 mM potassium phosphate buffer (pH 7.5) containing 0.2 M KCl or in 10 mM HEPES, adjusted to pH 7.5 with $Ca(OH)_2$. The reaction of dithionite-reduced MADH with amicyanin was studied in 10 mM potassium phosphate buffer (pH 7.5).

Spectral changes due to conversion of the quinol state of TTQ to the semiquinone state were measured at 443 nm. At this isosbestic point in the spectra of the semiquinone and the oxidized states of TTQ, the observed signal reflected only the conversion of the quinol to the semiquinone state (*5*). The molar extinction coefficient difference ($\Delta\varepsilon$) of 26200 M^{-1} cm^{-1} was used (*4*). The time courses of the reaction at 25 °C were fitted to single-exponential curves, and k_{obs} values were determined.

(ii) Electron Transfer in the Crystal. Single-crystal polarized absorption spectra were recorded using a Zeiss MPM 800 microspectrophotometer. Crystals were oriented with the principal optical directions parallel to the electric vector of the incident light, as previously described (*19, 41*). A single crystal was placed in a flow cell with quartz windows, in the presence of either its mother liquor or a replacing medium containing 0.5 mM methylamine. Reduction of TTQ was complete before the beginning of the spectrophotometric measurements. The pH dependence of electron distribution between the two redox centers was investigated by replacing the crystal surrounding medium with a new one at a different pH.

NMR Spectroscopy. For the assignment of the backbone amide resonances of reduced Cu amicyanin, HNCACB, HNCO, HN(CA)CO, CC(CO)NH, and $^{15}N-^{1}H$ HSQC spectra were acquired at 300 K on a Bruker Avance DMX 600 MHz NMR spectrometer equipped with a TCI-Z-GRAD ATM cryoprobe using a 2.5 mM ^{13}C- and ^{15}N-labeled sample of amicyanin, in 10 mM potassium phosphate (pH 6.8) and 1 mM sodium ascorbate and containing 6% D_2O for lock. Zn-substituted amicyanin was assigned on the basis of NOESY-$^{15}N-^{1}H$ HSQC and TOCSY-$^{15}N-^{1}H$ HSQC spectra on a 1.0 mM ^{15}N-labeled sample in the same buffer, but in the absence of ascorbate. These data were acquired using a TXI-Z-GRAD probe on the same spectrometer.

Chemical shift perturbation experiments were performed at 300 K on a Bruker DSX 750 MHz spectrometer using 0.20−0.25 mM samples of ^{2}H- and ^{15}N-labeled amicyanin in 20 mM potassium phosphate (pH 8.1), 1 mM methylamine, 1 mM sodium ascorbate, and 6% D_2O, to which aliquots of a concentrated stock of methylamine-reduced MADH were added. TROSY (*42*) spectra were acquired for 40 min to 4 h, depending on the concentration of MADH. In the indirect dimension, 80 complex points were acquired.

NMR Data Analysis. NMR data were processed using AZARA (http://www.bio.cam.ac.uk/azara/). Backbone assignment of Cu amicyanin was performed using the semi-automated procedure in Ansig-for-Windows (*43*). All non-proline residues were assigned except for Asn55 for which no signals were observed. Amides in Zn-substituted amicyanin were assigned by comparison with Cu amicyanin and confirmed by analysis of the NOESY-$^{15}N-^{1}H$ HSQC and TOCSY-$^{15}N-^{1}H$ HSQC spectra. TROSY spectra were compared using Ansig-for-Windows. Amicyanin resonances of the bound form could be assigned by comparison with the free form, except for several residues in the Zn-substituted form, which had shifted greatly. For these, a minimum perturbation was determined on the basis of the closest unassigned peak in the bound form. These were residues Val51, Val63, His96, Phe98, and Met99. For the assigned residues, the perturbation was quantified as $\Delta\delta_{avg} = [1/2(\Delta\delta N^2/25 + \Delta\delta H^2)]^{0.5}$, where $\Delta\delta N$ and $\Delta\delta H$ are the chemical shift changes of ^{15}N and ^{1}H nuclei, respectively, upon binding. Assignments, perturbations, and annotated HSQC spectra are included as Supporting Information (Tables S1−S3 and Figures S1 and S2).

RESULTS

Description of the Structure. The structure of *P. versutus* MADH has been reported previously (*25, 26*), and it remains largely unchanged when forming an ET complex with amicyanin (Figure 1). The enzyme forms a compact $\alpha_2\beta_2$

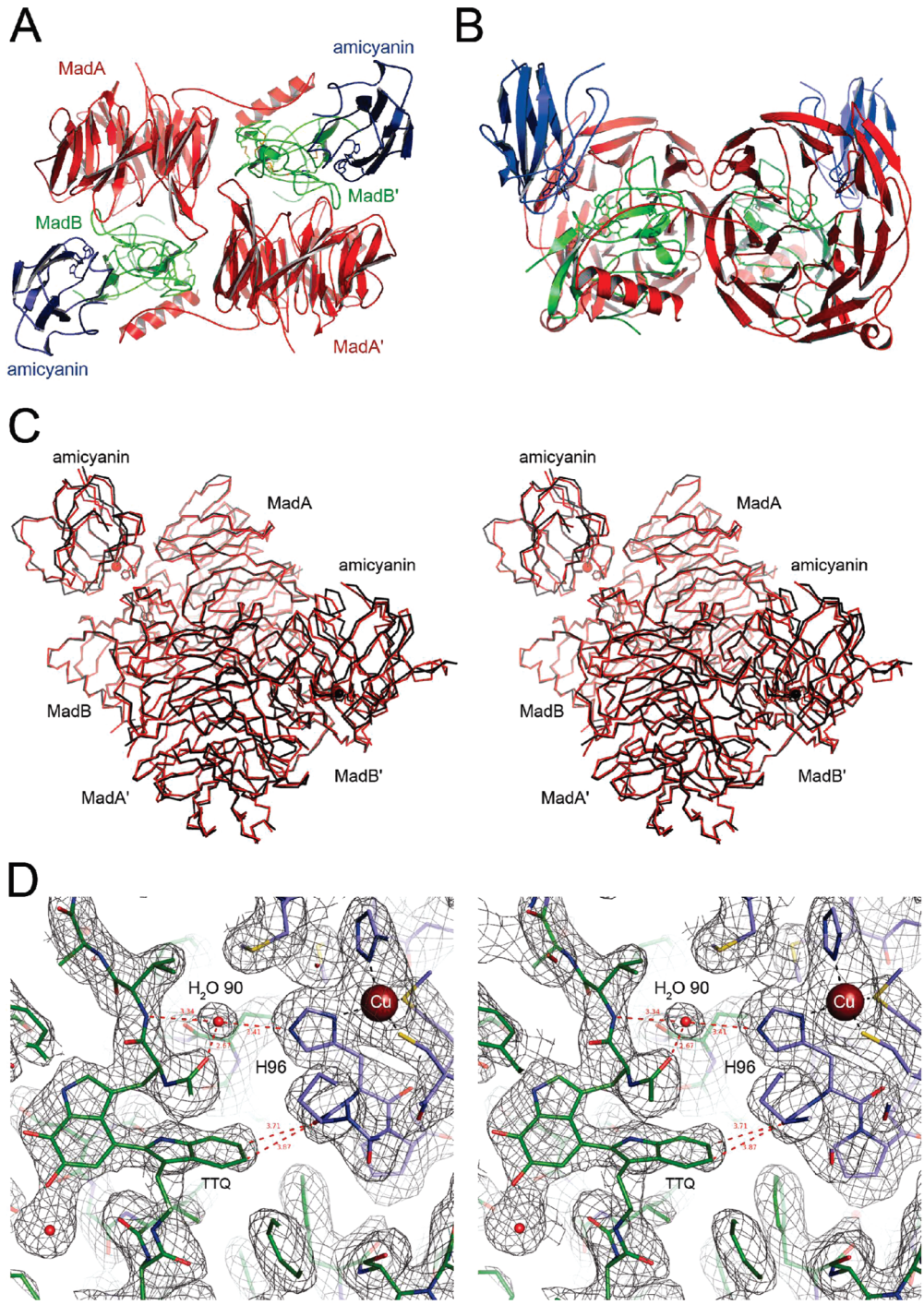

FIGURE 1: Structure of the MADH−amicyanin complex from *P. versutus*. (A) Top view of the overall complex with the large subunit MadA colored red, MadB colored green, and the redox partner amicyanin colored blue. (B) Side view of panel A. (C) Stereo representation of a superposition of the α-carbon atom traces of the MADH−amicyanin complexes from *P. versutus* (red) and *P. denitrificans* (black). (D) Stereo representation of the interface between amicyanin and MADH with a $2F_o - F_c$ electron density map contoured at 1σ. Carbon atoms of the subunits are colored by chain, green for MADH and blue for amicyanin.

heterotetramer consisting of a heavy (MadA, 395 amino acids, 43.3 kDa) and a light peptide chain (MadB, 131 amino acids, 14.2 kDa). The heavy (H) chain folds into a characteristic, seven-blade β-propeller domain and contains an N-terminal extension (residues 1−80) that wraps around the neighboring light (L) chain, fixing it to the tetrameric enzyme. It does not contain cofactors, and none of its residues is immediately involved in catalysis; however, because of its rigid structure, it forms a base for the light chain. The L subunit consists mainly of loop regions with only four β-strands, stabilized by a total of six disulfide bridges, containing the active site of the enzyme, a tryptophan tryptophylquinone moiety formed by Trp57 covalently linked to Trp108.

In the ET complex, amicyanin (Ami, 106 amino acids, 11.7 kDa) interacts with MADH close to the interface of the L and H subunit (for a list of contacts, see Table S4). A water molecule (W90) is located close to the N_ϵ atom of His96 of amicyanin and hydrogen bonded to the carbonyl oxygen of Ser56, next to the tryptophylquinone moiety in the adjacent L subunit (Figure 1D). It is observed only close to one of the two amicyanin molecules bound to MADH,

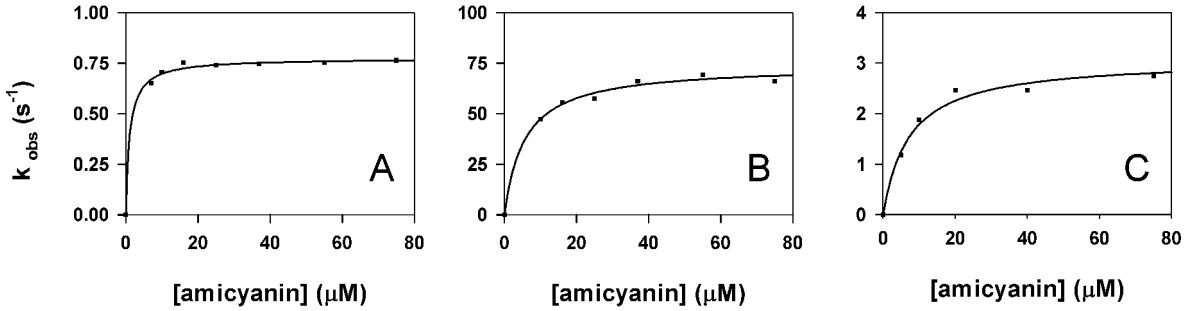

FIGURE 2: Rate constant profiles for the oxidation of MADH by amicyanin at 25 °C. (A) Methylamine-reduced MADH in 0.01 M Ca-HEPES (pH 7.5). (B) Methylamine-reduced MADH in 0.01 M phosphate (pH 7.5) with 0.2 M KCl. (C) Dithionite-reduced MADH in 0.01 M phosphate (pH 7.5). Solid lines represent the fitting to a hyperbolic function.

Table 2: Rate Constants (k_{obs})[a] of Amicyanin Reduction by MADH

reduction by	buffer	*P. versutus*	*P. denitrificans*
methylamine-reduced MADH	10 mM Ca-HEPES (pH 7.5)	0.77 ± 0.01 s^{-1}	~0.4 s^{-1}[b]
methylamine-reduced MADH	10 mM Na,K-phosphate (pH 7.5) and 0.2 M KCl	74 ± 2 s^{-1}	~160s^{-1}[c]
dithionite-reduced MADH	10 mM Na,K-phosphate (pH 7.5)	3.1 ± 0.2 s^{-1}	~9 s^{-1}[d]

[a] Values determined at 25 °C in the presence of saturating concentrations of amicyanin. [b] From ref *55*. [c] From ref *4*. [d] From ref *5*.

but it was modeled with an occupancy of 1.0. It suggests a path for ET coupling of the redox centers via Trp57−Ser56 O−W90−His96. An alternative pathway involves a through-space jump from the indole ring of Trp108 ($C_{\eta 2}$) to the oxygen atom of Pro95 and, via backbone atoms, to the imidazole of His96. Using the decay parameters proposed by Beratan et al. (*44*) and the distances determined in the structure presented here, similar electronic couplings are obtained for both pathways. An analogous water molecule had not been modeled in the original structure of the *P. denitrificans* binary complex (*2*), and the pathway via the analogous Trp ($C_{\eta 2}$) and Pro was proposed to be critical for ET from TTQ to copper (*5*). The pathway across a water molecule (W56) was, however, described in the higher-resolution structure of the ternary complex (*16*). Both pathways appear to provide good coupling of the redox centers. Further experiments are necessary to establish whether the connecting water is indeed relevant for ET.

Access for substrate to the active site of the enzyme is possible on the opposite side of the L subunit, where a substrate channel at the interface of L and H leads directly to the quinone site on Trp57.

Amicyanin Reduction by MADH. The rate of transfer of the first electron from methylamine-reduced *P. versutus* MADH to amicyanin has been reported to be increased by monovalent cations (*45, 46*), as in the case of the *P. denitrificans* system (*40*). Our data confirm a strong effect of KCl on the efficiency of ET from the methylamine-reduced TTQ (N-quinol) to amicyanin. In the absence of ions, the rate is nearly 2 orders of magnitude lower and similar to that observed for ET from the dithionite-reduced cofactor (Figure 2). A comparison of the rate constant values (k_{obs}) with the corresponding ones determined for the *P. denitrificans* system (Table 2) indicates that the functional properties of the two systems are similar.

In the crystal, MADH is reduced by the methylamine present in the surrounding medium. The rate is likely to be diffusion-limited but still too fast to be measured. In fact, within the time of spectrophotometric observation, the methylamine-derived electrons distribute themselves between

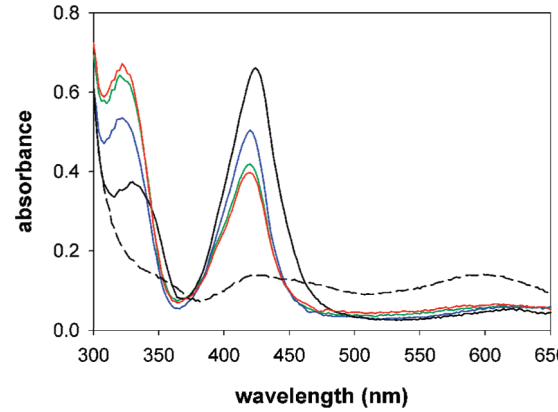

FIGURE 3: Single-crystal polarized absorption spectra of the amicyanin−MADH complex before (dashed line) and after (solid lines) reaction with methylamine at pH 6.5 (red), 7.0 (green), 7.5 (blue), and 9.5 (black).

TTQ and the amicyanin copper. As in the case of the *P. denitrificans* binary complex (*20*), the reversible distribution of electrons is pH-dependent, with a higher proportion of reduced copper as the pH increases. This is shown by the single-crystal polarized spectra reported in Figure 3. With increasing pH, the absorption of the reduced TTQ at 330 nm decreases with the concomitant increase of the absorption of the semiquinone form at 425 nm, indicative of ET to the copper.

Chemical Shift Perturbation Analysis. To study the complex of MADH and amicyanin in both redox states, Zn(II) amicyanin was used as a mimic for Cu(II) amicyanin. Cu(II) is paramagnetic, resulting in extensive broadening of resonances of many nuclei around the metal. It has been shown that metal substitution in blue copper proteins affects only the position of the ligand side chains and otherwise has very few structural effects. The rmsd of cobalt and copper amicyanin structures [PDB entries 1T5K (*47*) and 2OV0, respectively] is 0.55 Å for the backbone atoms. For Zn(II) forms of azurin (*48*) and pseudoazurin (*32*), similar results were found.

To investigate its site for binding to MADH in solution, amicyanin was enriched in ^{15}N, as well as ^{2}H for all

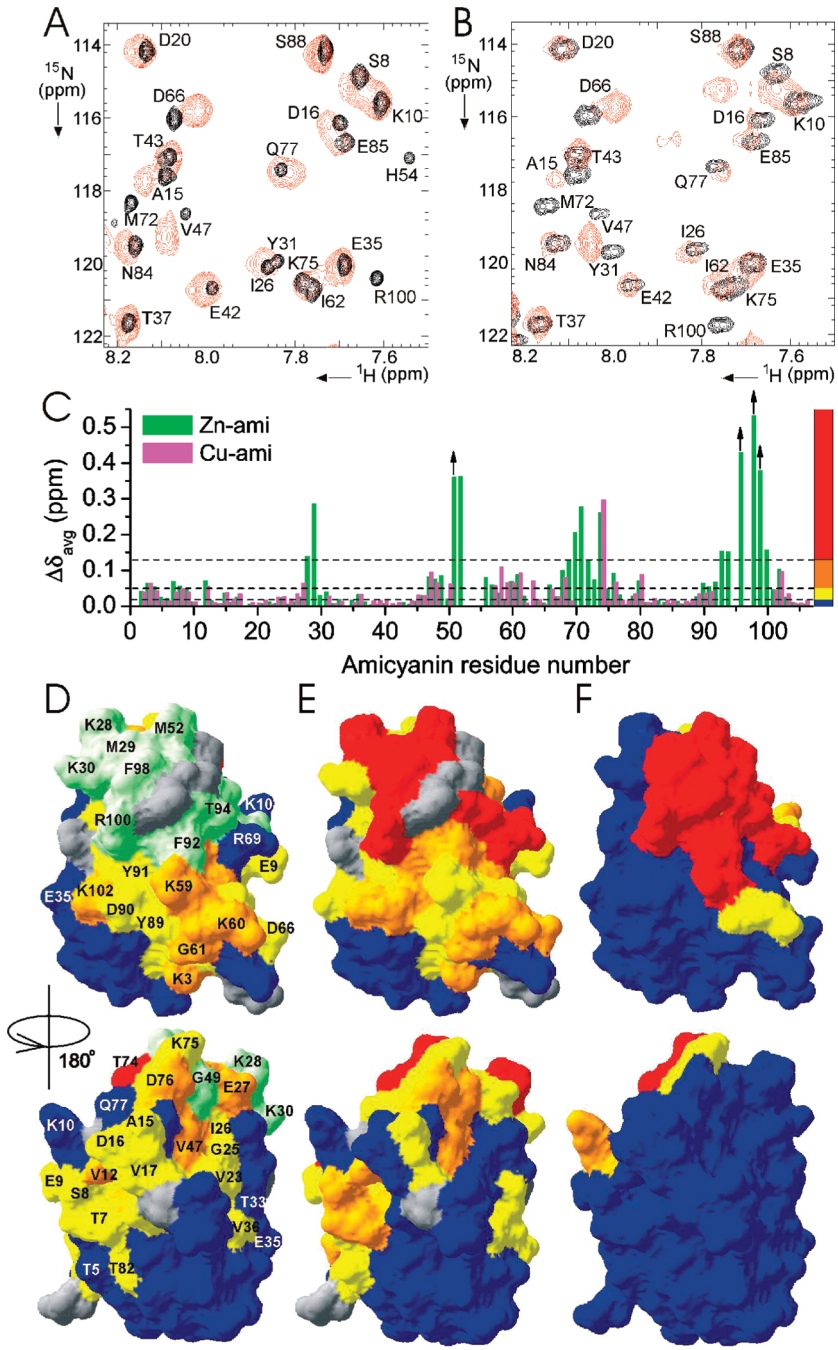

FIGURE 4: Chemical shift perturbation analysis. (A and B) Regions of the TROSY spectra of Cu(I) amicyanin (A) and Zn(II) amicyanin (B), free (black contours) and bound to MADH (red contours). The amicyanin−MADH protomer ratio was 1:5 (A) and 1:3 (B). (C) The $\Delta\delta_{avg}$ values are shown for all observed residues in Cu (magenta bars) and Zn (green bars) amicyanin. The arrows indicate residues for which only a minimum shift could be determined (see Experimental Procedures). (D and E) The $\Delta\delta_{avg}$ values have been mapped onto the surface representation of amicyanin using the color code indicated by the vertical bar at the right in panel C for Cu (D) and Zn (E) amicyanin. The residues that are not observed in the complex of MADH with Cu amicyanin are colored green. Unassigned residues and prolines are colored gray. The structure was taken from the crystal structure of the complex. (F) The residues of amicyanin have been colored according to the distance from MADH in the crystal structure of the complex, with residues with atoms within 4, 5, and 6 Å of MADH colored red, orange, and yellow, respectively, and other residues colored blue.

nonexchangeable protons. It is well established that in perdeuterated proteins the level of dipolar relaxation of the amide protons is strongly reduced, leading to sharp signals in the ^{15}N−^{1}H HSQC spectrum. In combination with TROSY-type experiments (*42*), this approach allows the observation of amicyanin amide resonances in the complex with MADH (Figure 4A,B). Upon titration with MADH, numerous resonances of amicyanin decrease in intensity and new resonances appear at 1.0 molar equiv of MADH protomers. For resonances with small perturbations, shifting signals were observed. It can be concluded that the exchange rate is slow to intermediate for most signals. The off-rate is estimated to be on the order of 250 s^{-1}.

A clear difference was observed between the titration performed with Cu(I) amicyanin and Zn(II)-substituted amicyanin. In the case of Cu(I) amicyanin, 19 resonances of amides close to the copper site disappeared upon addition of MADH without new resonances appearing. With Zn(II) amicyanin, the number of new peaks was equivalent to that of the signals that disappeared. This suggests that in the case

of Cu(I) amicyanin an exchange process takes place within the complex, leading to broadening of the resonances of amides close the copper. The possible reason for this behavior will be discussed later.

The formation of the complex has large effects on the chemical shifts of the amides. Figure 4 presents $\Delta\delta_{avg}$ values (panel C) and maps of the chemical shift perturbations on the structure of amicyanin in the complex, with the results for Cu(I) and Zn(II) amicyanin shown in panels D and E, respectively. In panel D, the missing residues are colored green. In the spectra of the complex of MADH with Zn(II)-substituted amicyanin, most peaks could be assigned by comparison of the free and bound forms. Five resonances of amides show such large chemical shift changes that they could not be assigned. However, they could be classified as "large perturbations" and are colored red in Figure 4E. The predominant effects are at the hydrophobic patch, surrounding the exposed copper ligand His96, a conserved part of the structure of blue copper proteins that is generally assumed to be the main interaction surface with ET partners. Weaker effects were observed around a patch of positive electrostatic surface potential located around Lys60. These regions can be identified as the interface for binding. Considerable perturbations are also observed on the other side of the protein. Many of these amides are buried, suggesting that these are secondary effects, caused by small structural changes inside the protein upon binding. This is confirmed by the crystal structure of the complex (see below). Except for the perturbation observed for Arg69 in Zn(II) amicyanin, the effects of binding are similar for the Cu(I) and Zn(II) amicyanins.

DISCUSSION

The MADH−amicyanin complexes of *P. denitrificans* and *P. versutus* are similar, with an overall root-mean-square deviation (rmsd) of 1.0 Å for all corresponding atoms in the crystal structures of the complexes (Figure 1C). This finding, together with the competence in ET, clearly indicates that in both cases a functional complex, and not merely a cocrystal, has been described. The structural resemblance is consistent with the high degree of sequence conservation (63, 74, and 98% for amicyanin and the MADH heavy and light chains, respectively) as well as with the similarity of the ET rates and the role of monovalent cations in the oxidation of methylamine-reduced MADH in solution. The lower efficiency in the ion activation agrees with the higher dissociation constants for ions reported for *P. versutus* MADH (*45*). These findings suggest that the subtle changes occurring within amicyanin upon its association with MADH, revealed by the new NMR data on the *P. versutus* complex, are likely to be a general feature of these systems.

The behavior of several resonances of amicyanin upon formation of a complex with MADH indicates that the dissociation rate constant for oxidized amicyanin is 250 s^{-1}, enabling a fast turnover of the enzyme, with the lifetime of the complex being 4 ms. Notwithstanding the transient nature of the complex, it is likely that MADH spends most time in the bound state, given the K_d in the low micromolar range (*6*) and the high protein concentrations in the periplasm.

Disappearance of Signals in the Cu(I) Amicyanin. Formation of a complex of Cu amicyanin with MADH results in the loss of signals from residues close to the copper. This is not observed for Zn-substituted amicyanin, suggesting that broadening of the signals is due to a process that can occur only in the Cu amicyanin. Two possibilities are considered.

First, a small fraction of Cu(II) amicyanin could cause extensive line broadening due to paramagnetic relaxation, provided electron exchange within as well as between the MADH−amicyanin complexes is sufficiently fast. Only in this case will all amicyanin molecules experience the broadening effect. Although the samples contained 1 mM methylamine and 1 mM sodium ascorbate to create a reducing environment, it is possible that during the long experiments the sample did not remain anaerobic. However, given the low rate constant values measured at low concentrations of monovalent ions, intracomplex ET is likely to be too slow in the NMR samples to result in line broadening.

Second, slow flipping of the His96 ring in the complex could lead to intermediate exchange of the amides surrounding the copper site. His96 is known to protonate and flip around pH 7 in free amicyanin and has been reported not to protonate in the complex between amicyanin and MADH from *P. denitrificans* due to steric hindrance observed in the crystal (*49*). However, the possibility that protonation and flipping occur in the complex in solution, leading to exchange broadening, cannot be excluded.

For Zn amicyanin, the line broadening is not observed. This result does not allow us to distinguish between the two explanations, because Zn amicyanin is neither redox active nor expected to exhibit protonation of His96.

Comparison between Solution and Crystal State Complexes. The chemical shift perturbations observed for amicyanin can be analyzed by comparison with the crystal structure of the complex. The most strongly affected residues are centered around Phe98 (Figure 4D,E), suggesting that this area of the amicyanin surface is part of the interface. This is in accordance with the crystal structure, which can be seen in Figure 4F, which shows the residues that are part of the interface of the complex colored red. It has been shown that mutagenesis of the equivalent Phe in the *P. denitrificans* complex has a large effect on the ET rate, which was attributed to a reduced level of electronic coupling between the redox sites (*50*). Figure 5 shows the interface of the complex with the NMR perturbations plotted on the backbone of amicyanin.

However, the area of residues exhibiting chemical shift perturbations is noticeably larger, involving the positive patch around Lys60 and numerous residues at the back of amicyanin. Two explanations have been provided to account for large areas of perturbations observed for ET complexes. First, the effects can be caused by small structural changes in the interface area that cause slight movements in secondary structure elements or changes in hydrogen bond networks, resulting in small structural changes far from the binding site (secondary perturbations). Second, the extended area can indicate that the complex in solution comprises a dynamic state as well as a well-defined state. In the dynamic state, other areas of the protein make contact with the partner, causing additional chemical shift perturbations, as observed for other proteins (*8, 51*). Although it is not straightforward to differentiate between the two possibilities, it is expected that a dynamic state affects surface residues, while the secondary perturbations can affect also residues in the interior

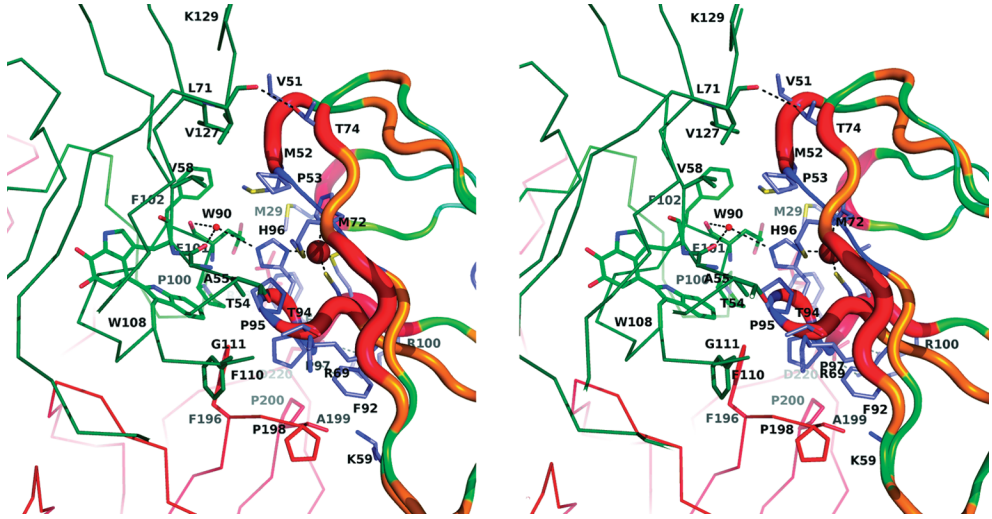

FIGURE 5: Stereo representation of the interface of the complex, showing MadA as a red, and MadB as a green C_α trace. The amicyanin backbone is shown as a tube with width and color coding according to the $\Delta\delta_{avg}$ value of the amide groups: cyan for $\Delta\delta_{avg} < 0.02$ ppm, green for $\Delta\delta_{avg} < 0.05$ ppm, orange for $\Delta\delta_{avg} < 0.13$ ppm, red for $\Delta\delta_{avg} > 0.13$ ppm, and blue for no data. Relevant side chains are shown as sticks, and the copper is shown as a sphere.

of the protein. Highly dynamic protein complexes exhibit small $\Delta\delta_{avg}$ values, compared to well-defined complexes (*52, 53*).

In the complex with MADH, amicyanin exhibits large $\Delta\delta_{avg}$ values, suggesting that the complex is mostly well-defined. This idea is supported by the fact that amicyanin is ordered in the crystal structure of the complex. Many perturbed amides are buried. Thus, it seems most likely that the extensive perturbations are of a secondary nature. The crystal structure offers the opportunity to check for structural changes involving residues with perturbed amides (Figure 6). The average rmsd for backbone atoms between free [PDB entry 1ID2 (*28*)] and MADH-bound amicyanin is 0.54 ± 0.06 Å (Figure 6A). This value and those given below represent the average (±standard deviation) over the three amicyanin molecules found in the asymmetric unit of the structure in PDB entry 1ID2, which was determined at 2.15 Å resolution. In the interface, the biggest differences are observed for the ligand loops, with 0.6 ± 0.1 and 1.0 ± 0.1 Å displacements for the carbonyl oxygens of Phe98 and Val51, respectively. The perturbations of residues 47−50 and 76 (Figure 6C) may be a consequence of changes around Val51, because of the hydrogen bond network that connects the buried Asn48 with Met52, Glu50, and Asp76.

Significant is the displacement of the β-strand that runs down from the interface, in the N-terminal direction, from Met72 to Ala67 (Figure 6B). Also, the loop from Asp66 to Lys60 has moved. The distance between the carbonyl oxygen of Val63 and the amide nitrogen of Lys3 has increased from 2.9 ± 0.2 to 3.8 Å, thus disrupting the hydrogen bond that connects the loop to the N-terminal residues (Figure 6D). These effects may be attributed to interactions of Arg69 with MADH, and they explain that perturbations are observed for the residues in this β-strand and residues 3 and 4, located far from the interface.

Also, the relatively mobile loop of residues 7−11 appears to have assumed a different average structure, perhaps because it is connected to Glu71 via ordered water molecules. This is in line with the perturbations observed for Thr7 and Ser8, as well as Ala80, which is connected via another water molecule to Ser8. This water (HOH numbers 104, 146, and 141 in the three chains in 1ID2 and HOH160 in chain A of 3C75) moves by 1 Å upon formation of a complex, increasing the distance to the carbonyl of Ser8 from 2.43 ± 0.04 to 3.2 Å (Figure 6E). This water is buried and more than 14 Å from the nearest atom of MADH. It is observed in all chains of the free amicyanin, but only in the A chain of the bound protein.

To check whether these effects of binding occur in both the *P. versutus* and *P. denitrificans* complexes, the crystal structures of MADH-bound (PDB entry 2MTA) and free (PDB entries 1AAN and 2OV0) amicyanin were also compared for the latter species. Interestingly, some effects described above are also observed for this complex. The average displacement of the O atom of Phe97 (*P. denitrificans* amicyanin counting is one less than *P. versutus*) is 0.5 Å in the same direction. The hydrogen bond between the O atom of Leu62 and the N atom of Lys2 is weakened (2.7 vs 2.9 Å), though not broken. The positive charge of Arg69 is conserved in *P. denitrificans* amicyanin as Lys68, and a similar rearrangement of the backbone is observed for this residue upon complex formation. The same is true for the binding changes around *P. denitrificans* Ser7. The structure around Ala50 is not disturbed, probably because of the lower steric hindrance with respect to the Val51 in *P. versutus* amicyanin. The water bridging Ser79 and Ser7 does not move significantly in the *P. denitrificans* complex, perhaps because it seems to be involved in a much stronger H-bond network than in *P. versutus*. Thus, while some binding effects are conserved, others, which are not, match structure differences between the two amicyanins.

CONCLUSION

The complex of *P. versutus* MADH and amicyanin has been studied both in the crystalline state and in solution. Deuteration of amicyanin, in combination with TROSY NMR spectroscopy, has allowed its observation in this large complex. The chemical shift perturbation map of amicyanin suggests that the complex in solution is similar to the crystal structure. Furthermore, very subtle changes in the hydrogen

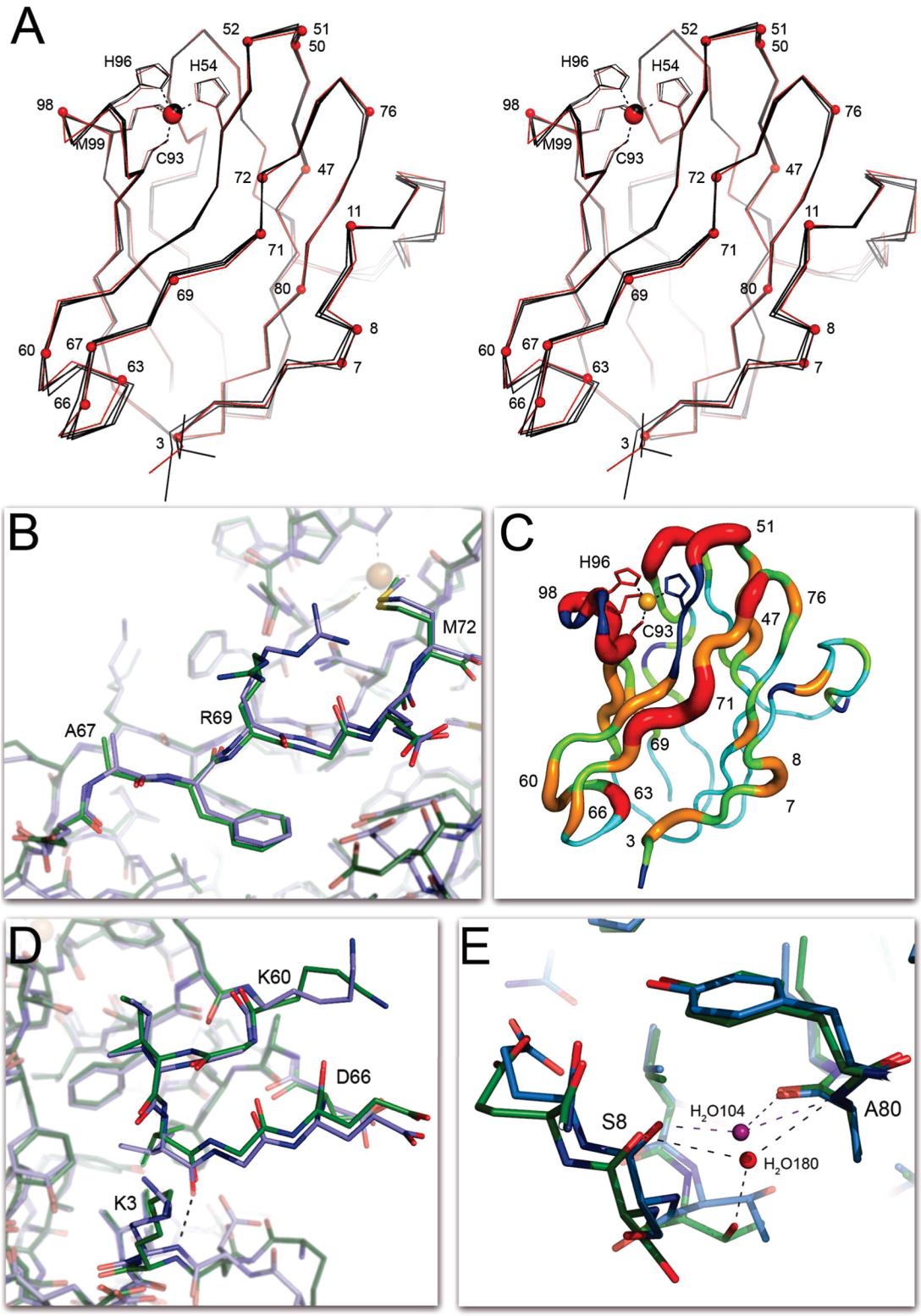

FIGURE 6: Perturbations in the amicyanin structure upon formation of the complex. (A) Stereo view of a superimposition of *P. versutus* amicyanin from the complex with MADH (red) with the three copies in the asymmetric unit of unbound amicyanin crystals (black, PDB entry 1ID2). Ligands to the copper ion as well as the protein residues mentioned in the Discussion are marked. (B) Detailed view of the β-strand from residue 67 to 72 with free amicyanin colored blue and the protein from the MADH complex green. Arg69 in this strand is involved in formation of the complex with MADH and may be the cause of the observed distortion. (C) Backbone trace of amicyanin with tube width and color coding according to the $\Delta\delta_{avg}$ value of the amide groups: cyan for $\Delta\delta_{avg} < 0.02$ ppm, green for $\Delta\delta_{avg} < 0.05$ ppm, orange for $\Delta\delta_{avg} < 0.13$ ppm, red for $\Delta\delta_{avg} > 0.13$ ppm, and blue for no data. (D) Detailed view of the loop region from residue 60 to 66. In the complex with MADH, this loop (green) adopts a conformation that disrupts a backbone hydrogen bond from Val63 to Lys3. (E) Detailed view of the area around Ser8, showing the displacement of a buried water molecule in the bound form of amicyanin (green; water molecule labeled as H_2O180).

bond network, which are observed in the crystal structure, but could have been discarded as insignificant, correlate with chemical shift perturbations of amides far from the interface. This combination of NMR and X-ray diffraction shows that even relatively weak binding of two proteins can result in structural effects deep inside a protein due to slight movements of secondary structure elements.

ACKNOWLEDGMENT

We are grateful to Ing. Johan Hollander for his help with the NMR experiments at 750 MHz.

SUPPORTING INFORMATION AVAILABLE

Assignments, annotated HSQC spectra, and chemical shift perturbation lists for Cu and Zn amicyanin, as well as a list of contacts between amicyanin and MADH (Tables S1−S4 and Figures S1 and S2). This material is available free of charge via the Internet at http://pubs.acs.org.

REFERENCES

1. Gray, K. A., Davidson, V. L., and Knaff, D. B. (1988) Complex formation between methylamine dehydrogenase and amicyanin from *Paracoccus denitrificans*. *J. Biol. Chem. 263*, 13987–13990.
2. Chen, L., Durley, R., Poliks, B. J., Hamada, K., Chen, Z., Mathews, F. S., Davidson, V. L., Satow, Y., Huizinga, E., Vellieux, F. M., and Hol, W. G. J. (1992) Crystal structure of an electron-transfer complex between methylamine dehydrogenase and amicyanin. *Biochemistry 31*, 4959–4964.
3. McIntire, W. S., Wemmer, D. E., Chistoserdov, A., and Lidstrom, M. E. (1991) A new cofactor in a prokaryotic enzyme: Tryptophan tryptophylquinone as the redox prosthetic group in methylamine dehydrogenase. *Science 252*, 817–824.
4. Bishop, G. R., and Davidson, V. L. (1995) Intermolecular electron transfer from substrate-reduced methylamine dehydrogenase to amicyanin is linked to proton transfer. *Biochemistry 34*, 12082–12086.
5. Brooks, H. B., and Davidson, V. L. (1994) Kinetic and thermodynamic analysis of a physiologic intermolecular electron-transfer reaction between methylamine dehydrogenase and amicyanin. *Biochemistry 33*, 5696–5701.
6. Davidson, V. L., Graichen, M. E., and Jones, L. H. (1993) Binding constants for a physiologic electron-transfer protein complex between methylamine dehydrogenase and amicyanin. Effects of ionic strength and bound copper on binding. *Biochim. Biophys. Acta 1144*, 39–45.
7. Ubbink, M., Ejdebäck, M., Karlsson, B. G., and Bendall, D. S. (1998) The structure of the complex of plastocyanin and cytochrome f, determined by paramagnetic NMR and restrained rigid-body molecular dynamics. *Structure 6*, 323–335.
8. Volkov, A. N., Worrall, J. A., Holtzmann, E., and Ubbink, M. (2006) Solution structure and dynamics of the complex between cytochrome c and cytochrome c peroxidase determined by paramagnetic NMR. *Proc. Natl. Acad. Sci. U.S.A. 103*, 18945–18950.
9. Vlasie, M. D., Fernandez-Busnadiego, R., Prudencio, M., and Ubbink, M. (2008) Conformation of pseudoazurin in the 152 kDa electron transfer complex with nitrite reductase determined by paramagnetic NMR. *J. Mol. Biol. 375*, 1405–1415.
10. Leys, D., Basran, J., Talfournier, F., Sutcliffe, M. J., and Scrutton, N. S. (2003) Extensive conformational sampling in a ternary electron transfer complex. *Nat. Struct. Biol. 10*, 219–225.
11. Ashikawa, Y., Fujimoto, Z., Noguchi, H., Habe, H., Omori, T., Yamane, H., and Nojiri, H. (2006) Electron transfer complex formation between oxygenase and ferredoxin components in Rieske nonheme iron oxygenase system. *Structure 14*, 1779–1789.
12. Dai, S., Friemann, R., Glauser, D. A., Bourquin, F., Manieri, W., Schürmann, P., and Eklund, H. (2007) Structural snapshots along the reaction pathway of ferredoxin-thioredoxin reductase. *Nature 448*, 92–96.
13. Chen, L., Mathews, F. S., Davidson, V. L., Tegoni, M., Rivetti, C., and Rossi, G. L. (1993) Preliminary crystal structure studies of a ternary electron transfer complex between a quinoprotein, a blue copper protein, and a *c*-type cytochrome. *Protein Sci. 2*, 147–154.
14. Chen, L., Durley, R. C., Mathews, F. S., and Davidson, V. L. (1994) Structure of an electron transfer complex: Methylamine dehydrogenase, amicyanin, and cytochrome *c*551i. *Science 264*, 86–90.
15. Sukumar, N., Chen, Z. W., Ferrari, D., Merli, A., Rossi, G. L., Bellamy, H. D., Chistoserdov, A., Davidson, V. L., and Mathews, F. S. (2006) Crystal structure of an electron transfer complex between aromatic amine dehydrogenase and azurin from *Alcaligenes faecalis*. *Biochemistry 45*, 13500–13510.
16. Mathews, F. S., Chen, Z.-W., Durley, R. C. E., Davidson, V. L., Jones, L. H., Graichen, M. E., Hosler, J. H., Merli, A., Brodersen, D. E., and Rossi, G. L. (1998) Structural Research on the Methylamine Dehydrogenase Redox Chain of *Paracoccus denitrificans*, in *Biological Electron-Transfer Chains: Genetics, Composition and Mode of Operation* (Canters, G. W., and Vijgenboom, E., Eds.) pp 129−146, Kluwer Academic Publishers, Dordrecht, The Netherlands.
17. Davidson, V. L., and Jones, L. H. (1996) Electron transfer from copper to heme within the methylamine dehydrogenase-amicyanin-cytochrome c-551i complex. *Biochemistry 35*, 8120–8125.
18. Davidson, V. L. (2000) What controls the rates of interprotein electron-transfer reactions. *Acc. Chem. Res. 33*, 87–93.
19. Merli, A., Brodersen, D. E., Morini, B., Chen, Z., Durley, R. C., Mathews, F. S., Davidson, V. L., and Rossi, G. L. (1996) Enzymatic and electron transfer activities in crystalline protein complexes. *J. Biol. Chem. 271*, 9177–9180.
20. Ferrari, D., Merli, A., Peracchi, A., Di Valentin, M., Carbonera, D., and Rossi, G. L. (2003) Catalysis and electron transfer in protein crystals: The binary and ternary complexes of methylamine dehydrogenase with electron acceptors. *Biochim. Biophys. Acta 1647*, 337–342.
21. Ferrari, D., Di Valentin, M., Carbonera, D., Merli, A., Chen, Z. W., Mathews, F. S., Davidson, V. L., and Rossi, G. L. (2004) Electron transfer in crystals of the binary and ternary complexes of methylamine dehydrogenase with amicyanin and cytochrome c551i as detected by EPR spectroscopy. *J. Biol. Inorg. Chem. 9*, 231–237.
22. Hyun, Y. L., Zhu, Z., and Davidson, V. L. (1999) Gated and ungated electron transfer reactions from aromatic amine dehydrogenase to azurin. *J. Biol. Chem. 274*, 29081–29086.
23. Chandrasekar, R., and Klapper, M. H. (1986) Methylamine dehydrogenase and cytochrome c552 from the bacterium W3A1. *J. Biol. Chem. 261*, 3616–3619.
24. Chistoserdov, A. Y., McIntire, W. S., Mathews, F. S., and Lidstrom, M. E. (1994) Organization of the methylamine utilization (mau) genes in *Methylophilus methylotrophus* W3A1-NS. *J. Bacteriol. 176*, 4073–4080.
25. Vellieux, F. M., Huitema, F., Groendijk, H., Kalk, K. H., Frank Jzn, J., Jongejan, J. A., Duine, J. A., Petratos, K., Drenth, J., and Hol, W. G. (1989) Structure of quinoprotein methylamine dehydrogenase at 2.25 Å resolution. *EMBO J. 8*, 2171–2178.
26. Huizinga, E. G., van Zanten, B. A., Duine, J. A., Jongejan, J. A., Huitema, F., Wilson, K. S., and Hol, W. G. (1992) Active site structure of methylamine dehydrogenase: Hydrazines identify C6 as the reactive site of the tryptophan-derived quinone cofactor. *Biochemistry 31*, 9789–9795.
27. Kalverda, A. P., Wymenga, S. S., Lommen, A., van de Ven, F. J., Hilbers, C. W., and Canters, G. W. (1994) Solution structure of the type 1 blue copper protein amicyanin from *Thiobacillus versutus*. *J. Mol. Biol. 240*, 358–371.
28. Romero, A., Nar, H., Huber, R., Messerschmidt, A., Kalverda, A. P., Canters, G. W., Durley, R., and Mathews, F. S. (1994) Crystal structure analysis and refinement at 2.15 Å resolution of amicyanin, a type I blue copper protein, from *Thiobacillus versutus*. *J. Mol. Biol. 236*, 1196–1211.
29. Jørgensen, L. E., Ubbink, M., and Danielsen, E. (2004) Amicyanin metal-site structure and interaction with MADH: PAC and NMR spectroscopy of Ag-, Cd-, and Cu-amicyanin. *J. Biol. Inorg. Chem. 9*, 27–38.
30. van Houwelingen, T., Canters, G. W., Stobbelaar, G., Duine, J. A., Frank, J. J., and Tsugita, A. (1985) Isolation and characterization of a blue copper protein from *Thiobacillus versutus*. *Eur. J. Biochem. 153*, 75–80.
31. Sambrook, J., Fritsch, E. F., and Maniatis, T. (1989) *Molecular cloning: A laboratory manual*, Cold Spring Harbor Laboratory Press, Plainview, NY.

32. Prudencio, M., Rohovec, J., Peters, J. A., Tocheva, E., Boulanger, M. J., Murphy, M. E., Hupkes, H. J., Kosters, W., Impagliazzo, A., and Ubbink, M. (2004) A caged lanthanide complex as a paramagnetic shift agent for protein NMR. *Chemistry 10*, 3252–3260.
33. van Wielink, J. E., Frank, J., and Duine, J. A. (1990) Methylamine dehydrogenase from *Thiobacillus versutus*, in *Methods in Enzymology*, pp 235−241, Academic Press, New York.
34. Otwinowski, Z., and Minor, W. (1996) Processing of X-ray diffraction data collected in oscillation mode, in *Methods in Enzymology*, pp 307−326, Academic Press, New York.
35. Collaborative Computational Project Number 4 (1994) The CCP4 suite: Programs for protein crystallography. *Acta Crystallogr. D50*, 760–763.
36. Chen, L., Doi, M., Durley, R. C., Chistoserdov, A. Y., Lidstrom, M. E., Davidson, V. L., and Mathews, F. S. (1998) Refined crystal structure of methylamine dehydrogenase from *Paracoccus denitrificans* at 1.75 Å resolution. *J. Mol. Biol. 276*, 131–149.
37. Jones, T. A., Zou, J. Y., Cowan, S. W., and Kjeldgaard, M. (1991) Improved methods for building protein models in electron density maps and the location of errors in these models. *Acta Crystallogr. A47* (2), 110–119.
38. Emsley, P., and Cowtan, K. (2004) Coot: Model-building tools for molecular graphics. *Acta Crystallogr. A60*, 2126–2132.
39. Brünger, A. T., Adams, P. D., Clore, G. M., DeLano, W. L., Gros, P., Grosse-Kunstleve, R. W., Jiang, J. S., Kuszewski, J., Nilges, M., Pannu, N. S., Read, R. J., Rice, L. M., Simonson, T., and Warren, G. L. (1998) Crystallography & NMR system: A new software suite for macromolecular structure determination. *Acta Crystallogr. D54*, 905–921.
40. Bishop, G. R., Brooks, H. B., and Davidson, V. L. (1996) Evidence for a tryptophan tryptophylquinone aminosemiquinone intermediate in the physiologic reaction between methylamine dehydrogenase and amicyanin. *Biochemistry 35*, 8948–8954.
41. Pearson, A. R., Mozzarelli, A., and Rossi, G. L. (2004) Microspectrophotometry for structural enzymology. *Curr. Opin. Struct. Biol. 14*, 656–662.
42. Pervushin, K., Riek, R., Wider, G., and Wüthrich, K. (1997) Attenuated T2 relaxation by mutual cancellation of dipole-dipole coupling and chemical shift anisotropy indicates an avenue to NMR structures of very large biological macromolecules in solution. *Proc. Natl. Acad. Sci. U.S.A. 94*, 12366–12371.
43. Helgstrand, M., Kraulis, P., Allard, P., and Hard, T. (2000) Ansig for Windows: An interactive computer program for semiautomatic assignment of protein NMR spectra. *J. Biomol. NMR 18*, 329–336.
44. Beratan, D. N., Betts, J. N., and Onuchic, J. N. (1991) Protein electron transfer rates set by the bridging secondary and tertiary structure. *Science 252*, 1285–1288.
45. Gorren, A. C., and Duine, J. A. (1994) The effects of pH and cations on the spectral and kinetic properties of methylamine dehydrogenase from *Thiobacillus versutus*. *Biochemistry 33*, 12202–12209.
46. Gorren, A. C., de Vries, S., and Duine, J. A. (1995) Binding of monovalent cations to methylamine dehydrogenase in the semiquinone state and its effect on electron transfer. *Biochemistry 34*, 9748–9754.
47. Carrell, C. J., Wang, X., Jones, L., Jarrett, W. L., Davidson, V. L., and Mathews, F. S. (2004) Crystallographic and NMR investigation of cobalt-substituted amicyanin. *Biochemistry 43*, 9381–9389.
48. Nar, H., Huber, R., Messerschmidt, A., Filippou, A. C., Barth, M., Jaquinod, M., van de Kamp, M., and Canters, G. W. (1992) Characterization and crystal structure of zinc azurin, a by-product of heterologous expression in *Escherichia coli* of *Pseudomonas aeruginosa* copper azurin. *Eur. J. Biochem. 205*, 1123–1129.
49. Zhu, Z., Cunane, L. M., Chen, Z., Durley, R. C., Mathews, F. S., and Davidson, V. L. (1998) Molecular basis for interprotein complex-dependent effects on the redox properties of amicyanin. *Biochemistry 37*, 17128–17136.
50. Davidson, V. L., Jones, L. H., and Zhu, Z. (1998) Site-directed mutagenesis of Phe 97 to Glu in amicyanin alters the electronic coupling for interprotein electron transfer from quinol methylamine dehydrogenase. *Biochemistry 37*, 7371–7377.
51. Ubbink, M., and Bendall, D. S. (1997) Complex of plastocyanin and cytochrome c characterized by NMR chemical shift analysis. *Biochemistry 36*, 6326–6335.
52. Worrall, J. A., Liu, Y., Crowley, P. B., Nocek, J. M., Hoffman, B. M., and Ubbink, M. (2002) Myoglobin and cytochrome b_5: A nuclear magnetic resonance study of a highly dynamic protein complex. *Biochemistry 41*, 11721–11730.
53. Worrall, J. A., Reinle, W., Bernhardt, R., and Ubbink, M. (2003) Transient protein interactions studied by NMR spectroscopy: The case of cytochrome c and adrenodoxin. *Biochemistry 42*, 7068–7076.
54. Weiss, M. S., and Hilgenfeld, R. (1997) On the use of the merging R factor as a quality indicator for X-ray data. *J. Appl. Crystallogr. D55*, 203–205.
55. Davidson, V. L., and Sun, D. (2003) Evidence for substrate activation of electron transfer from methylamine dehydrogenase to amicyanin. *J. Am. Chem. Soc. 125*, 3224–3225.

BI7023749